

# Electronic Supplementary Information

## **Tunable one-step double functionalization of graphene based on fluorographene chemistry**

Demetrios D. Chronopoulos,<sup>a</sup> Miroslav Medved',<sup>a</sup> Georgia Potsi,<sup>a</sup> Ondřej Tomanec,<sup>a</sup> Magdalena Scheibe,<sup>a</sup> and Michal Otyepka<sup>a,b\*</sup>

<sup>a</sup> Faculty of Science, Regional Centre of Advanced Technologies and Materials, Palacký University in Olomouc, Šlechtitelů 27, 783 71 Olomouc, Czech Republic

<sup>b</sup> Department of Physical Chemistry, Faculty of Science, Palacký University in Olomouc, 17. listopadu 1192/12, 771 46 Olomouc, Czech Republic

# 1 Experimental studies

## 1.1 Materials

Fluorinated graphite (GF) (C:F 1:1.1, >61 wt. %F), organolithium reagents (2-Thienyllithium solution and n-Butyllithium solution) and anhydrous tetrahydrofuran (THF) were purchased from Sigma-Aldrich. All reagents were used as received without further purification.

## 1.2 Experimental section

A typical reaction for the preparation of single functionalized graphene derivatives:

62 mg of GF were suspended in 10 mL of anhydrous THF with the aid of sonication for 4 h and the mixture was degassed and flushed with nitrogen. Subsequently, the appropriate amount of an organolithium reagent (4, 2 or 1 equivalents – eq.) was added dropwise to the above suspension and the reaction mixture was stirred under nitrogen for 18 h, at room temperature. Then, the unreacted organolithium reagent was quenched with ethanol (EtOH) and the solution was centrifuged for 10 min in 20000 rounds per min. Finally, the black precipitate was suspended consecutively in water, ethanol and dichloromethane several times and the desired material was collected after centrifugation.

Double functionalization of FG in one-step:

According to XPS measurements, it was found that 4 eq. of organolithium reagent was the effective amount for the almost quantitative elimination of fluorine atoms. Hence, 2 eq. of 2-Thienyllithium and 2 eq. of n-Butyllithium were added dropwise to a GF suspension (62 mg of GF in 10 mL of anhydrous THF) simultaneously. Afterwards, the above described typical procedure was followed.

Control experiments:

2 eq. of one of the organolithium reagents (e.g. 2-Thienyllithium, n-Butyllithium) were added dropwise to a GF suspension (62 mg of GF in 10 mL of anhydrous THF) and the reaction mixture was stirred under nitrogen for 18 h. Then, 2 eq. of the other organolithium reagent were added dropwise to the reaction mixture and the new mixture left for stirring under nitrogen for 18 h. For the quenching and washing the above described typical procedure was followed.

### 1.3 Instrumentation

X-ray photoelectron spectroscopy (XPS) was carried out with a PHI VersaProbe II (Physical Electronics) spectrometer using an Al K $\alpha$  source (15 kV, 50 W). The obtained data were evaluated with the MultiPak (Ulvac - PHI, Inc.) software package. Concerning the conditions of the measurements, every spot size of the measured materials was 100  $\mu\text{m}$  and three different spots were measured for each sample. The used take-off angle was 45°, providing thus depth information  $>3$  nm.

FT-IR spectra were recorded on an iS5 FTIR spectrometer (Thermo Nicolet) using the Smart Orbit ZnSe ATR accessory. Briefly, a droplet of an ethanolic dispersion of the relevant material was placed on a ZnSe crystal and left to dry and form a film. Spectra were acquired by summing 52 scans recorded under a nitrogen gas flow through the ATR accessory. ATR and baseline correction were applied to the collected spectra.

Raman spectra were recorded on a DXR Raman microscope using the 455 nm excitation line of a diode laser.

Electron microscopy images were obtained with a JEOL 2010 TEM equipped with a LaB6 type emission gun operating at 160 kV. STEM-HAADF (high-angle annular dark-field imaging) analyses for EDS (energy-dispersive X-ray spectroscopy) mapping of elemental distributions on the products were performed with a FEI Titan HRTEM operating at 80 kV. For these analyses, a droplet of an aqueous dispersion of the material at a concentration of  $\sim 0.1$  mg mL $^{-1}$  was deposited on a carbon-coated copper grid and slowly dried at ambient temperature for 24 h to reduce its content of adsorbed water.

AFM images were obtained in the amplitude modulated semicontact mode on an NT-MDT NTegra system equipped with a VIT-P AFM probe with the amplitude set point set to 71% of the free amplitude, a scanning speed of 0.5 Hz per line for all pictures, and using fresh cleaved muscovite mica.

Thermogravimetric analysis (TGA) with evolved gas analysis (EGA) was performed using a Netzsch STA 449C Jupiter thermo-microbalance coupled with a QMS 403C Aëolos quadrupole mass spectrometer. Measurements were carried out in an  $\alpha$ -Al $_2$ O $_3$  open crucible under N $_2$  flow. A temperature program from 40 to 1000 °C with heating rate of 10 °C min $^{-1}$  was used. Before each experiment, the crucible was heated to 1340 °C and then cooled to room temperature.

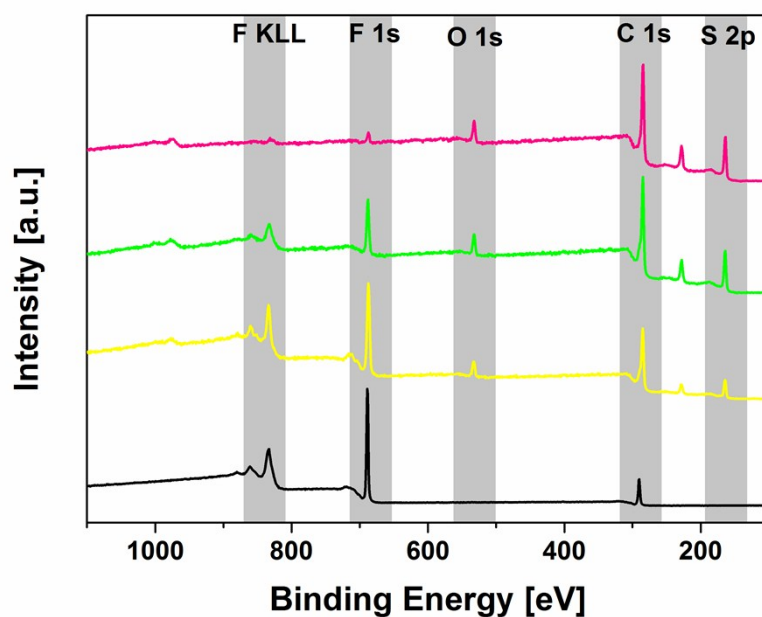


**Figure S1.** XPS survey spectra of G-4Th (treatment of FG with 4 eq. of 2-ThLi) (pink), G-Th (treatment of FG with 2 eq. of 2-ThLi) (green), G-1Th (treatment of FG with 1 eq. of 2-ThLi) (yellow) and pristine GF (black).

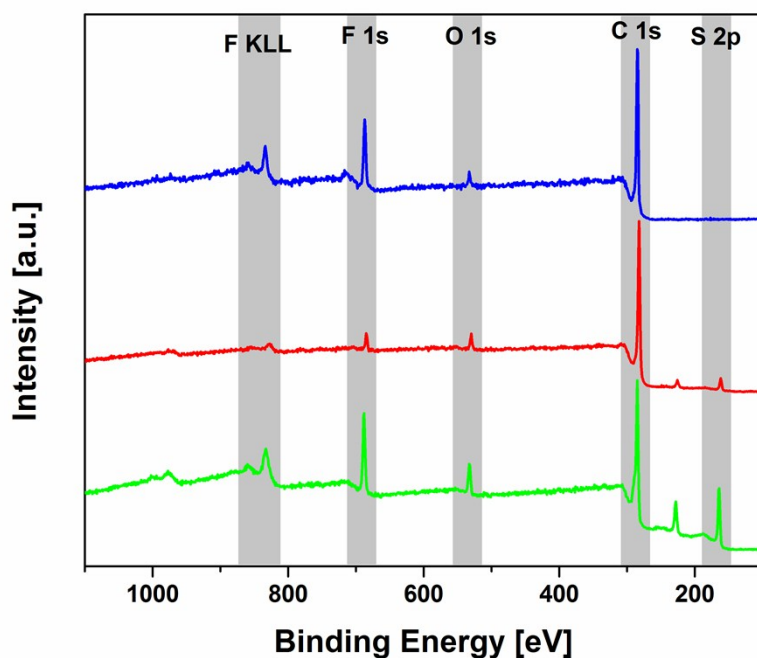


**Figure S2.** XPS survey spectra of G-Th (green), G-Bu (blue) and G-Th/Bu (red).

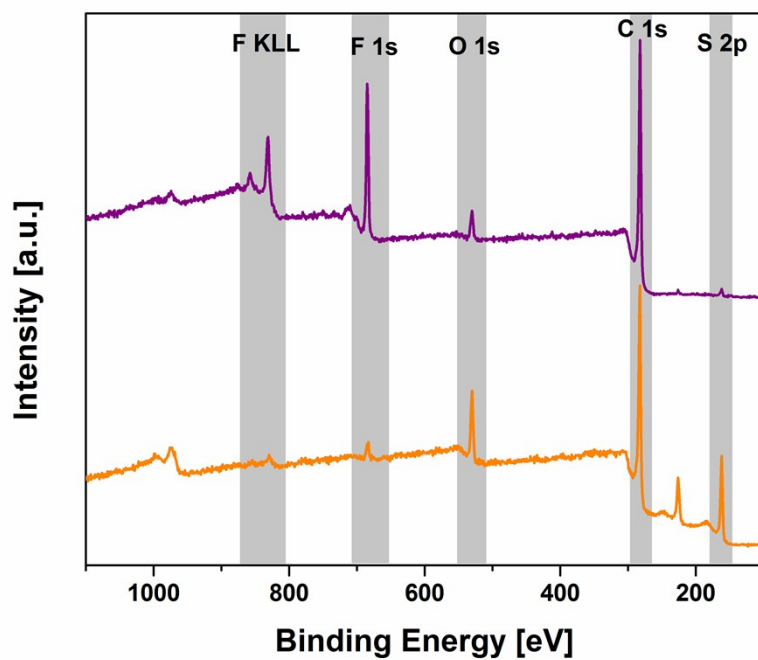


**Figure S3.** XPS survey spectra of G-Th(Bu) (orange) and G-Bu(Th) (purple).

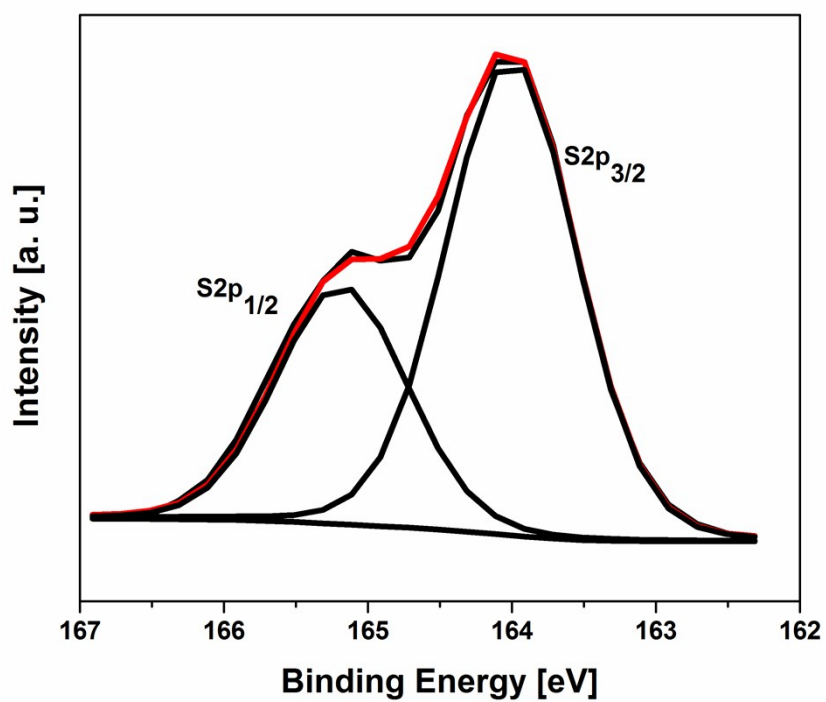


**Figure S4.** High resolution S 2p XPS spectrum of G-Th.

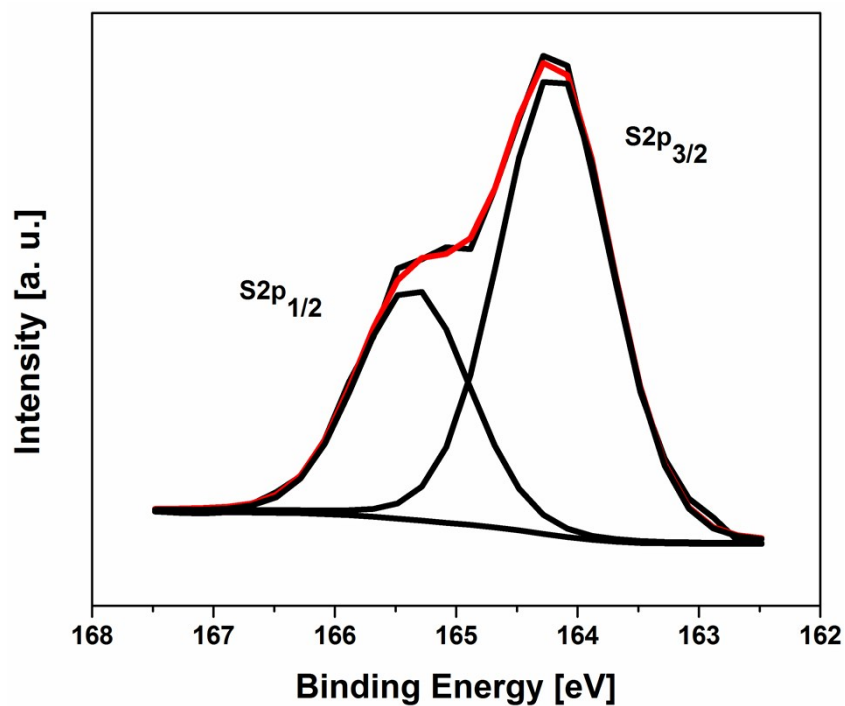


**Figure S5.** High resolution S 2p XPS spectrum of G-Th/Bu.

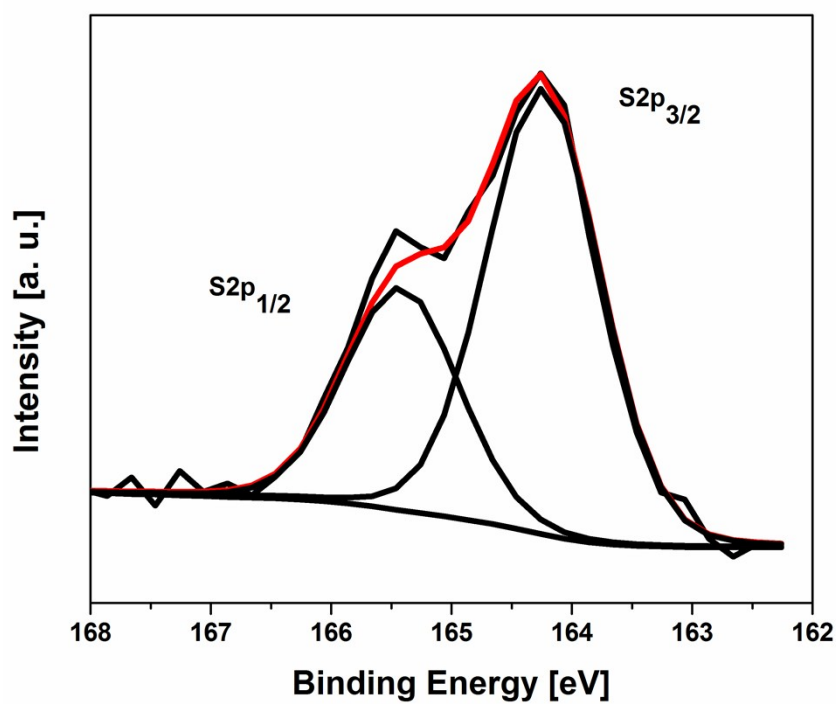


**Figure S6.** High resolution S 2p XPS spectrum of G-Th(Bu).

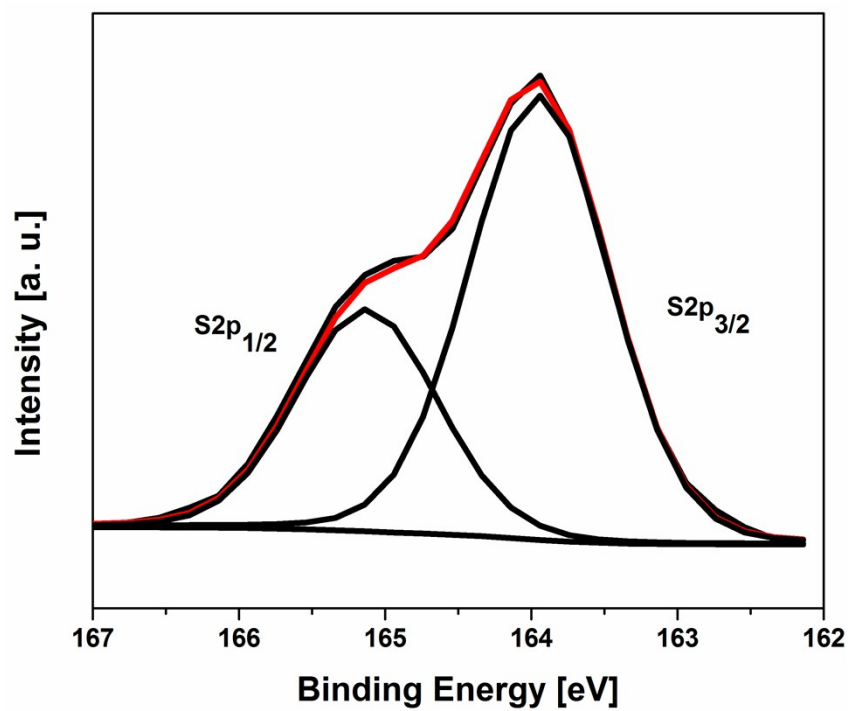


**Figure S7.** High resolution S 2p XPS spectrum of G-Bu(Th).

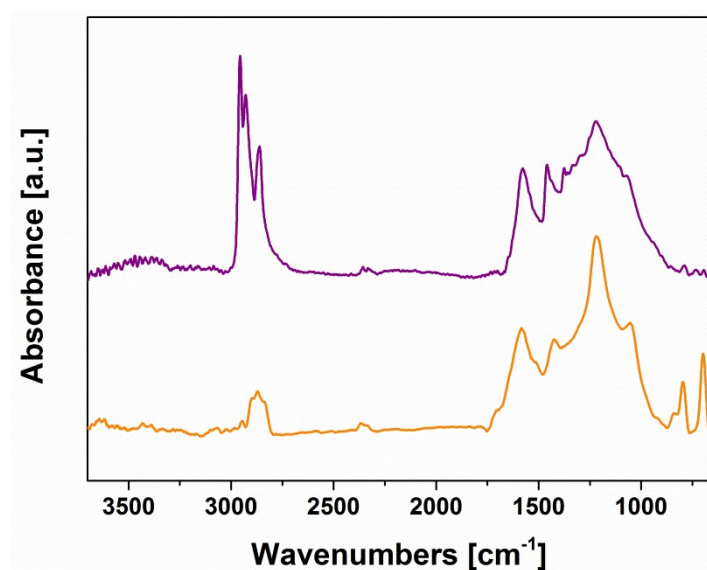


**Figure S8.** FT-IR spectra of graphene derivatives G-Th(Bu) (orange) and G-Bu(Th) (purple).

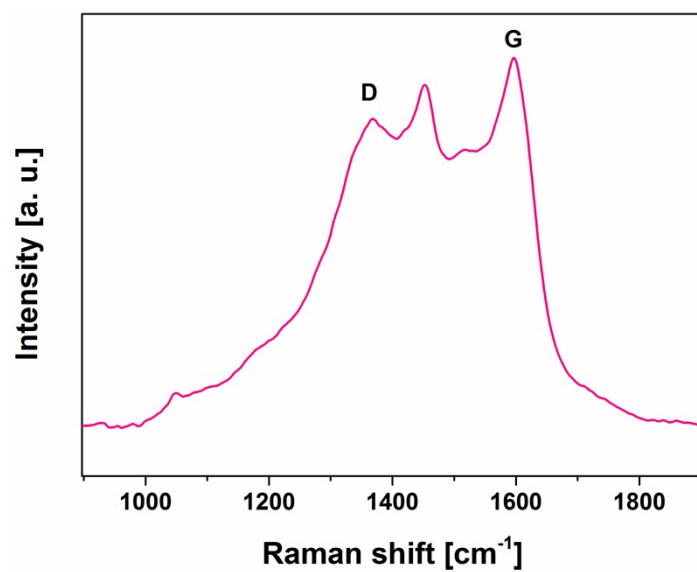


**Figure S9.** Raman spectrum of G-4Th, after treatment of FG with 4 eq. of 2-ThLi.

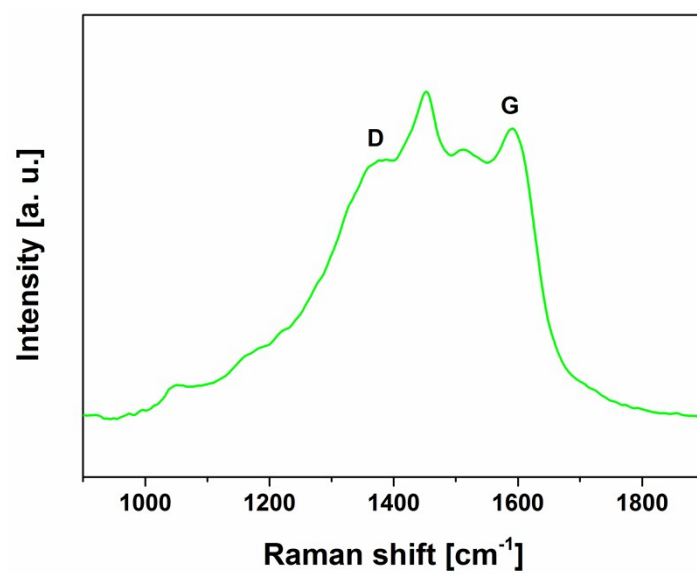


**Figure S10.** Raman spectrum of G-Th, after treatment of FG with 2 eq. of 2-ThLi.

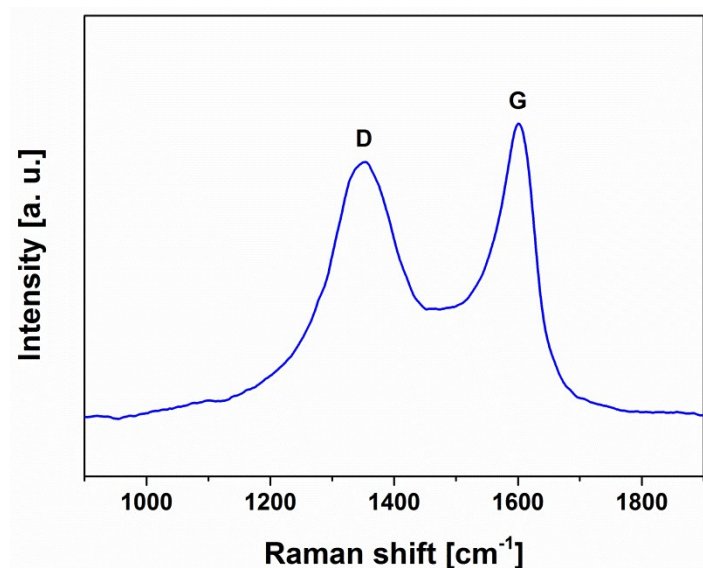


**Figure S11.** Raman spectrum of G-Bu (blue).

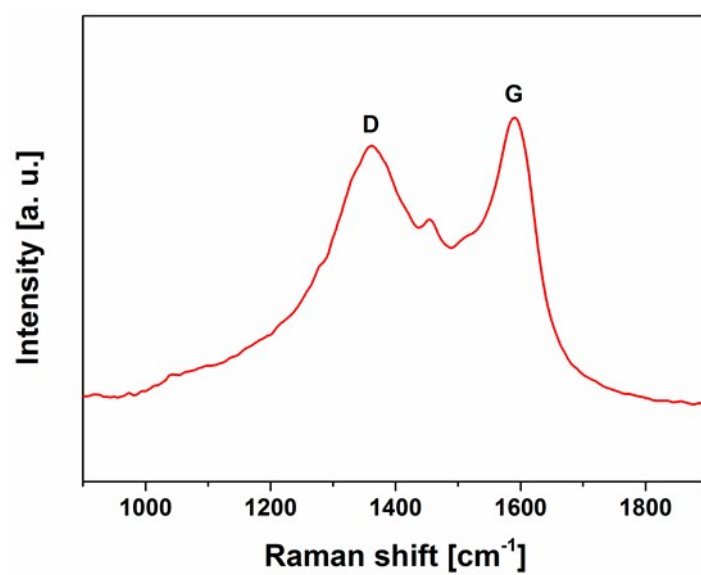


**Figure S12.** Raman spectrum of G-Th/Bu (red).

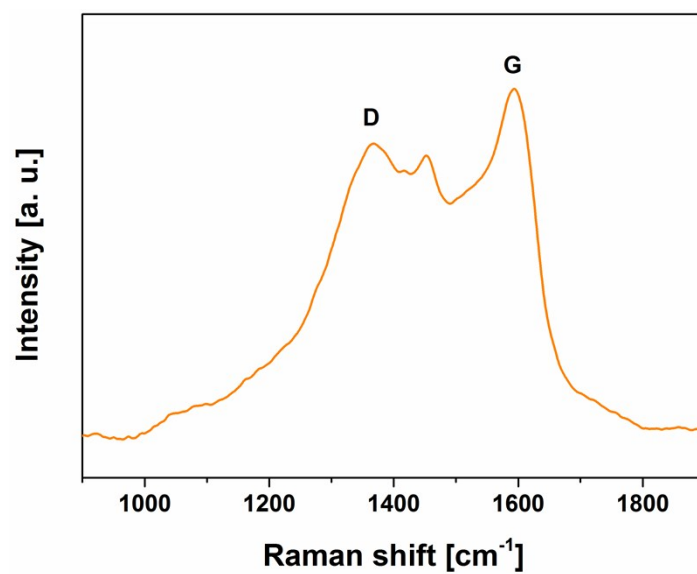


**Figure S13.** Raman spectrum of G-Th(Bu) (orange).

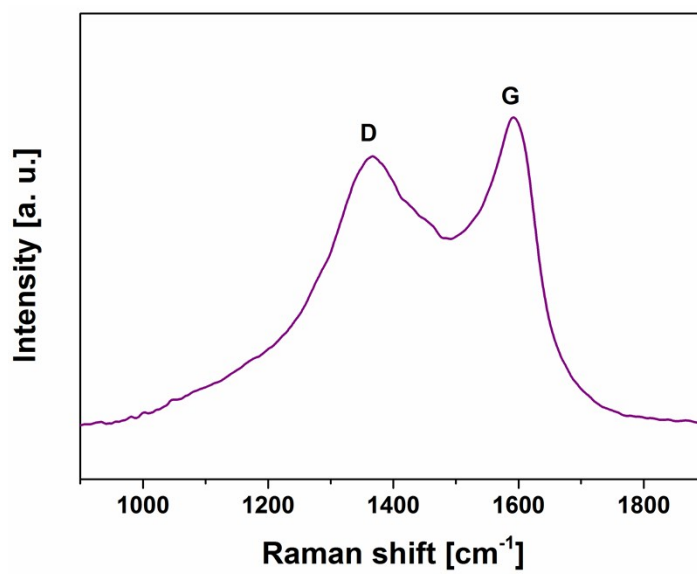


**Figure S14.** Raman spectrum of G-Bu(Th) (purple).

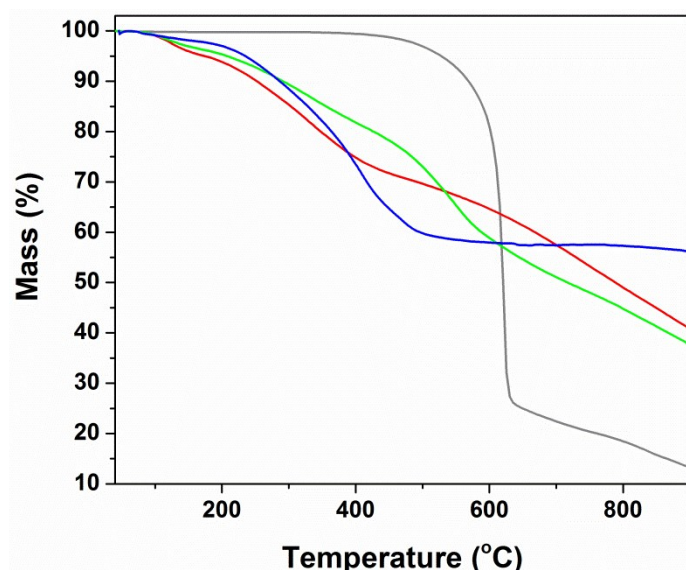


**Figure S15.** A) TGA graphs of GF (grey), G-Th (green), G-Bu (blue) and G-Th/Bu (red). All the TGA graphs were obtained under  $N_2$  atmosphere. The continuous mass loss for G-Th and G-Th/Bu can possibly be related to inability to repair the graphene lattice after the loss of the organic addends (Th), whereas in the case of G-Bu and G-Bu(Th) the lattice remains more compact and/or some self-repairing process takes place. Let us note that the similar stability of the material above 500 °C was also observed in the case of other alkylated graphene derivatives.

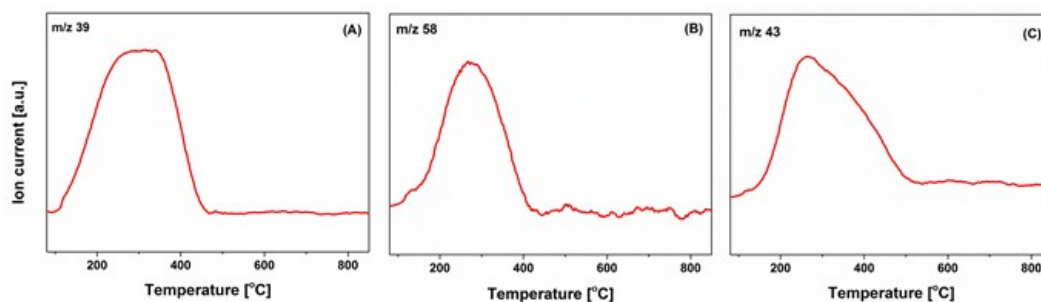


**Figure S16.** Ion current vs. temperature curve obtained with a mass spectrometer during the thermal degradation study (TGA-MS) of the G-Th/Bu. (A) and (B) are attributed to thiophene ring and (C) to butyl fragments.

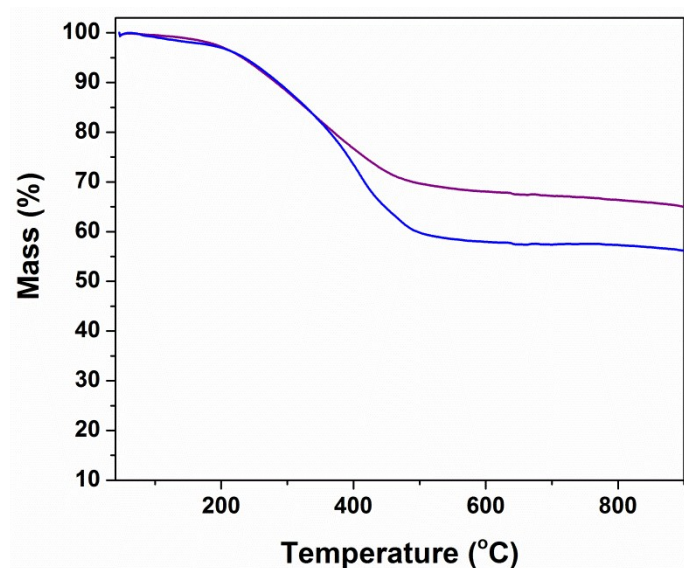


**Figure S17.** TGA graphs of G-Bu (blue) and G-Bu(Th) (purple). All the TGA graphs were obtained under  $N_2$  atmosphere.

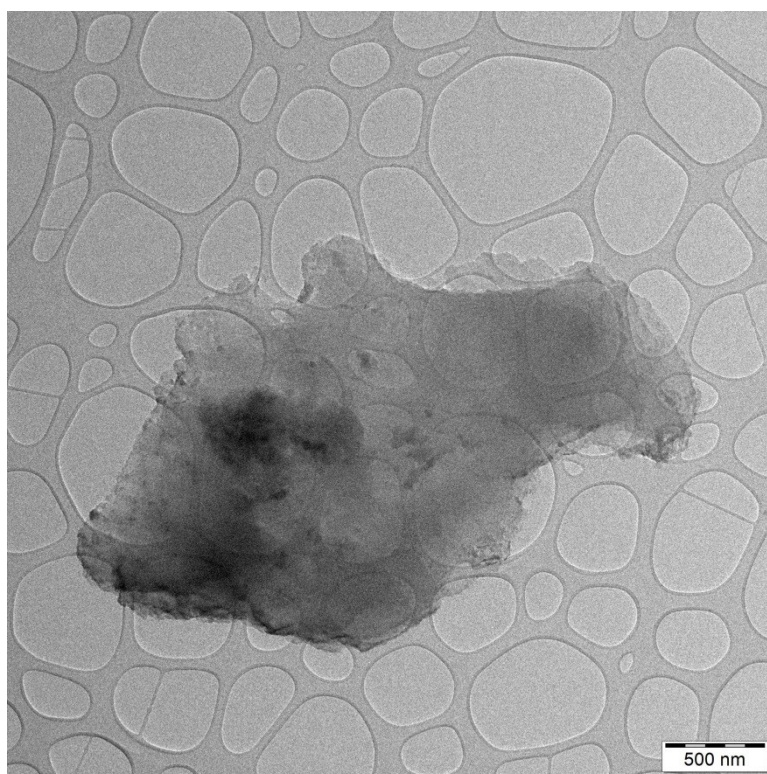


**Figure S18.** TEM image of G-Th/Bu.

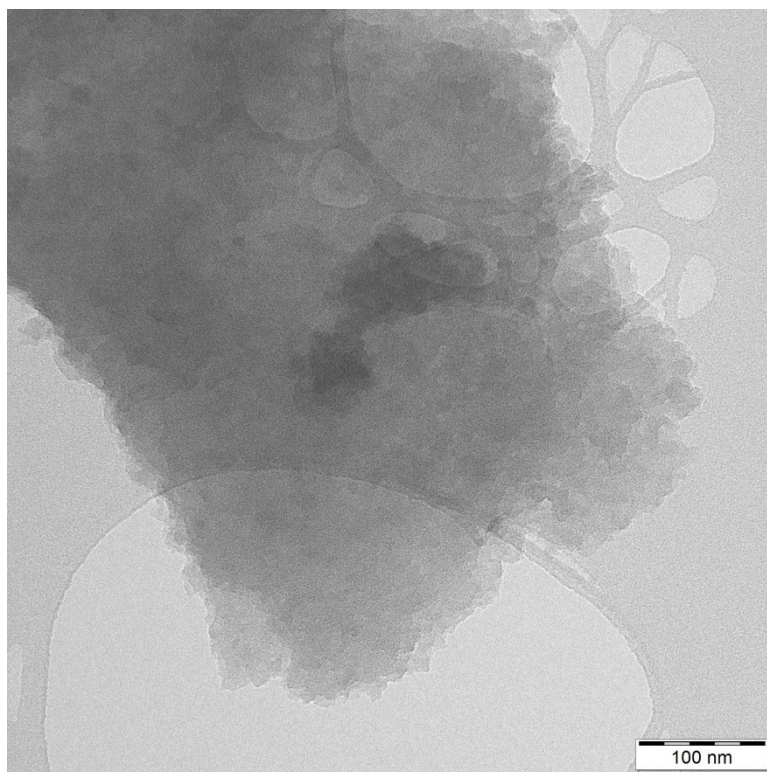


**Figure S19.** TEM image of **G-Th(Bu)**.

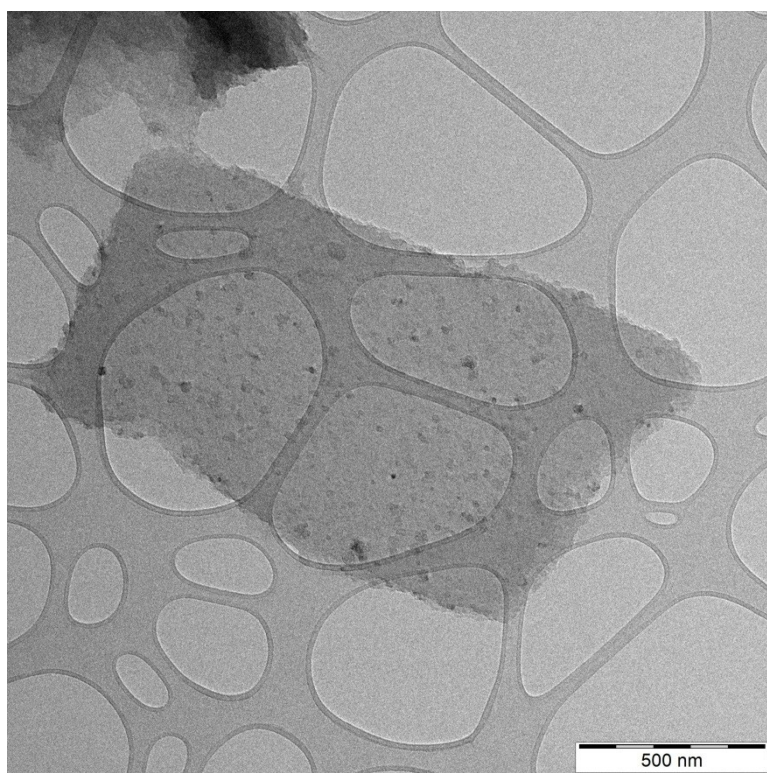


**Figure S20.** TEM image of **G-Bu(Th)**.

**Table S1.** Elemental composition of chemically modified graphene derivatives, after the reaction of FG with 4 eq., 2 eq. and 1 eq. of 2-ThLi as obtained from the XPS analyses (wide scan XPS spectra).

	Atomic percentage [%]				
	C 1s (283 eV)	N 1s (400 eV)	O 1s (531 eV)	F 1s (686 eV)	S 2p (165 eV)
<b>G-4Th</b>	75.2	0.5	8.3	2.7	13.3
<b>G-Th</b>	71.5	0.3	6.1	12.4	9.7
<b>G-1Th</b>	61.0	0.6	6.2	26.6	5.6

**Table S2.** Elemental composition of chemically modified graphene derivatives and pristine GF as obtained from the XPS analyses (wide scan XPS spectra).

	Atomic percentage [%]				
	C 1s (283 eV)	N 1s (400 eV)	O 1s (531 eV)	F 1s (686 eV)	S 2p (165 eV)
<b>G-Th</b>	71.5	0.3	6.1	12.4	9.7
<b>G-Bu</b>	82.5	0.5	3.1	13.9	-
<b>G-Th/Bu</b>	89.0	0.6	5.1	2.6	2.7
<b>G-Th(Bu)</b>	76.0	0.6	10.7	2.6	10.1
<b>G-Bu(Th)</b>	79.0	0.5	4.3	15.4	0.8
Graphite fluoride (GF)	43.5	0.24	0.24	55.7	-

## 2 Computational studies

Density functional theory (DFT) calculations of nucleophilic strengths and binding energies of nucleophiles on different types of partially functionalized FG (pFG) substrates were performed by  $\omega$ B97X-D method in combination with the 6-31+G(d) basis set. The solvent effects were included by using the universal continuum solvation model based on solute electron density (SMD). Whereas the structures of nucleophiles (Fig. 4a,b) as well as that of partially fluorinated ovalene (a finite-size model of pFG) were fully relaxed in geometry optimizations, to mimic the semilocal rigidity of FG sheets, partially functionalized FG structures (Figure 4c-e) as well as pFGs functionalized with Bu and Th groups were obtained by constrained geometry optimizations keeping the edge carbon atoms fixed. Figure S21 shows the optimized structures and the partial charges on carbon atoms in the defluorinated region of (a) pFG, (b) G-Bu, and (c) G-Th in THF. The total charge in the defluorinated area calculated as a sum of indicated partial charges indicates the decreasing electrophilic strength in the order partially fluorinated graphene (+0.44e) > butylated FG (+0.16e) > thiophenyl-FG (-1.24e).

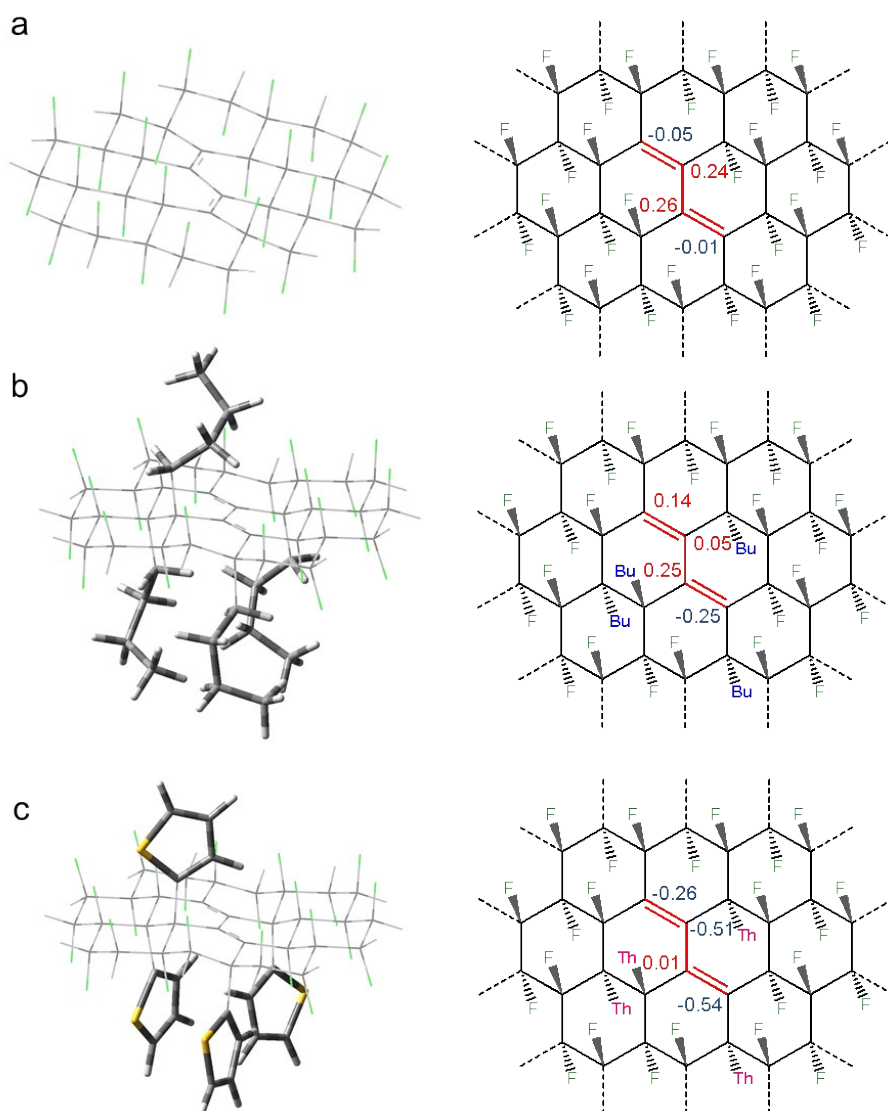


**Figure S21.** Optimized structures and Mulliken charges on carbon atoms in the defluorinated region of pFG, (b) G-Bu, and (c) G-Th in THF obtained at the  $\omega$ B97X-D/6-31+G(d)/SMD level of theory.

The shape and the volume of addends can (aside from their nucleophilicity and the electrophilicity of the substrates) affect their binding ability to the substrate mainly due to possible sterical hindrance with already bound groups, especially in the final phase of the reaction (which was not modeled theoretically). In fact, the sterical hindrance is very probably a key factor putting limitations on the degree of functionalization. Although it is by no means straightforward to evaluate separately the volume effects, their role can be qualitatively assessed by looking for relationships between the binding energies of nucleophiles and the molecular volumes of the substrates in the gas phase and solvent (THF). In Table S3 we report the molar volumes of Bu/Th anions and substrates corresponding to structures shown in Fig. 4. The observations can be summarized as follows:

- The molar volumes of Bu and Th anions are similar, i.e., the latter is larger only by 4 and 2 % in the gas phase and THF, respectively. Therefore, they differ more by structural flexibility than by their volume.

- The molar volumes of the partially fluorinated graphene model (FG) in the gas phase and THF are practically the same (as could be expected for the system with atomic addends) and they are notably smaller compared to G-Bu and G-Th. As in this case the sterical hindrance between Bu/Th anions and the substrate is small, the differences in binding energies can safely be attributed to different nucleophilic strengths of the agents.
- The molar volume of model G-Bu is notably larger than that of model G-Th (having the same number of addends as G-Bu) in the gas phase, BUT slightly smaller in THF. This is apparently related to the fact that non-polar chains of Bu groups tend to rearrange in polar solvents becoming more compact compared to the gas phase. The molar volume of G-Th is much less affected by the solvent, yet more than that of FG.
- If the binding energies were ruled by the molecular volumes, it could be anticipated that the relative binding energies of Bu and Th anions would be significantly affected by the change of the environment, in particular in the case the G-Bu substrate. Indeed, in this case, the binding of G-Bu...Bu is stronger than that of G-Bu...Th in the gas phase by -35.1 (= -46.1 - (-11.0)) kcal/mol to be compared with -29.6 kcal/mol (= -8.0 - (+21.6) kcal/mol) in THF, suggesting that the differences in binding are somewhat less pronounced in THF. However, the difference between these relative values can be rationalized in terms of higher stabilization of the Bu anion in THF (its solvation energy is by -4.9 kcal/mol more negative than that of Th).
- Also, the binding energies of G-Bu...Bu are consistently more negative compared to G-Th...Bu (by -7.1 and -6.3 kcal/mol in the gas phase and THF, respectively), despite the relative changes of molar volumes of the substrates when moving from the gas phase to solvent. The similarity of these values supports the hypothesis that the binding is ruled predominantly by nucleophilicity of agents and electrophilicity of the substrate rather than sterical effects, at least in the early phases of the reaction.

**Table S3** Molar volumes (in bohr<sup>3</sup>/mol) of Bu/Th anions and substrates corresponding to structures shown in Fig. 4 calculated by the Monte-Carlo method of calculating molar volume based on 0.001 e/bohr<sup>3</sup> density envelope at the  $\omega$ B97X-D/6-31+G(d)/SMD level of theory.

System	Molar volume	
	Gas phase	THF
Bu anion	847.5	898.0
Th anion	882.8	914.4
FG	4262.8	4261.6
G-Bu	7570.1	5971.6
G-Th	6745.9	6307.7